FOCUSING AN ARBITRARY RF PULSE AT A DISTANCE USING TIME REVERSAL TECHNIQUES

Sun K. Hong[a], Biniyam T. Taddese[b], Zachary B. Drikas[a], Steven M. Anlage[b] and Tim D. Andreadis[a]

[a]HPM Section, U.S. Naval Research Laboratory, Washington, DC, 20375, USA, [b]Department of Physics, University of Maryland, College Park, MD, 20742, USA

Abstract: In this paper we demonstrate the use of a time reversal (TR) technique to effectively focus an arbitrary RF pulse at a remote location from a single feed aperture for directed energy applications. The TR focusing is achieved by backing the aperture with a reverberating cavity, whose multipath environment enables the reconstruction of the aperture field distribution needed for directing the energy to the target location. Here, we use the impulse response between the target location and the time-reversal mirror (TRM) located inside the cavity to enable the effective transmission of arbitrary RF pulses, which are convolved with the time-reversed impulse response before transmission. The demonstration is carried out both numerically and experimentally for various RF pulses. The results show good temporal and spatial focusing at the target location. This approach could be an efficient selective "beamforming" method for directed energy, where it only requires a single feed and the impulse response between the TRM and target location or direction to effectively deliver an RF pulse of choice within an ultra-wide bandwidth of the impulse response.

Keywords: time reversal; temporal and spatial focusing; directed energy, high power microwave; beamforming

1. Introduction

Due to the inherent spatial and temporal focusing capability, the use of electromagnetic time reversal (TR) has been investigated for various applications [1-14]. Taking advantage of the time-reversal symmetry in the wave equation, TR techniques utilize the concept of a time reversal mirror (TRM), which captures the wave emitted from a source and retransmits the time-reversed version of the captured signal back into the propagation medium allowing for the waves to converge back to the source both in space and time.

Depending on the application, a TRM can consist of multi-element array or a single antenna in order to realize TR focusing. For applications such as wireless communications [2-7] or sensors [10-12] in rich scattering or high multipath environment, a single element TRM was shown to be sufficient for TR focusing, although a TRM consisting of multiple antennas could improve TR focusing [7].

The potential use of a TRM for directed energy applications was demonstrated by utilizing a reverberating box with an aperture to focus an RF pulse at a distance outside the box [14]. It is possible to spatiotemporally focus microwaves from an aperture without the use of a TRM. For instance, a beamforming technique that gives control over the angular and temporal dimensions of an array pattern has been proposed [16]. Besides, wavefront shaping has been used to focus waves

spatiotemporally through complex scattering media [17]. However, the use of TRM may be preferred due to its minimal computational cost to achieve focusing. The spatiotemporal focusing capability of TRMs has already been investigated in depth [18,19].

In this paper, we present a technique to effectively focus an arbitrary RF pulse at a desired distant location from a single feed aperture over an ultra-wide bandwidth. This technique uniquely builds upon the work in Ref. [14], by enabling the use of an RF pulse with an arbitrary shape. Here, the time-reversed impulse response between a given target location and the TRM is convolved with an arbitrary RF pulse, such that when transmitted through the TRM port, the RF pulse will focus at the target location as it exits the cavity through the aperture. Our method suggests that it requires only the impulse response between the ports to effectively apply TRM with an arbitrary pulse at any frequency within the bandwidth of the impulse response, which essentially is limited only by the bandwidth of the feed and the source electronics. Using a TRM in a leaky reverberating cavity with an aperture, we demonstrate the focusing of an RF pulse at a given target location using both numerical simulations and measurements. TRMs have already been applied for optimum beamforming [20]; our approach explores selective beamforming using a reverberating cavity.

The results show that the focusing takes place both in time and space, indicating that an arbitrary RF pulse can be effectively delivered to the target location using our single feed TRM. This approach provides an efficient selective "beamforming" method for directed energy over an ultra-wide bandwidth, where it requires a single feed and only the impulse response (pre-stored or obtained on the fly) between the TRM and target location or direction to effectively deliver an RF pulse of choice within the bandwidth of the impulse response (Figure 1a). Due to the spatial reciprocity of this problem, this approach also shows that TR focusing can be done at a specific location in an enclosed system with a finite number of entry ports or apertures as shown in Figure 1b. One potential
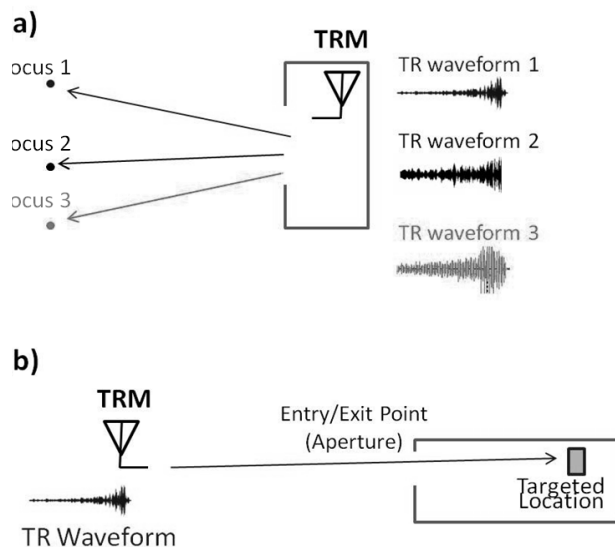

Figure 1. Potential directed energy applications using TR techniques: a.) Use of different TR waveforms to focus energy at different locations or directions, and b.) Use of TR waveforms to reconstruct a strong pulse at a key location inside an enclosure
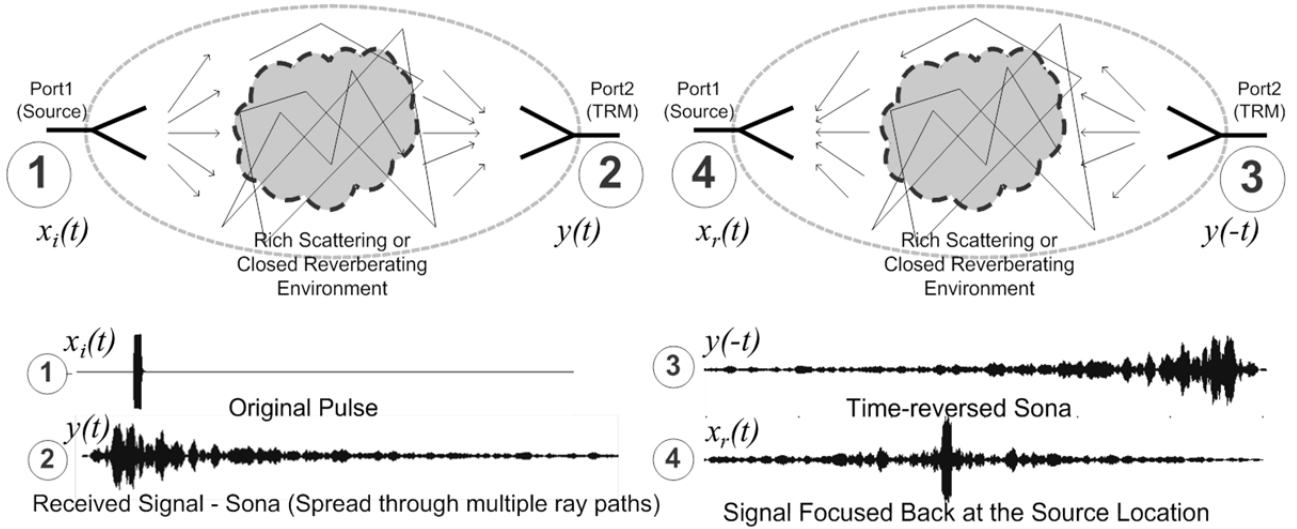
Figure 2. Overview of four-step process of TRM

application would be to target electronic devices inside an enclosure through the use of nonlinear time reversal [22]. Another example would be indoor to outdoor communications, where windows or openings can be regarded as apertures backed by rich scattering indoor environment.

2. Approach

2.1. TRM Process and TRM in a Leaky Box

The conventional TRM process involves four steps as shown in Fig. 2. First, Port1(source) transmits a pulsed waveform, $x_i(t)$, and Port 2 (receiver, which consists of a single or multiple antenna elements) records the response, $y(t)$, that is spread in time due to the signals following multiple ray paths. The recorded signal is then time-reversed and re-transmitted from Port 2. The time-reversed signal will then "backpropagate" to Port 1, focusing (both in time and space) waves back to the source, thereby generating a signal $x_r(t)$ that is very close to a time-reversed version of the original pulse.

Recently, Davy *et al*. have applied a TRM with an aperture backed by a reverberating box to focus a broadband RF pulse outside the box, at some distance away from the aperture [10]. As shown in Figure 3, the focusing is made possible due to the reverberating box that allows much of the signal $x_i(t)$ transmitted from Port 1 to enter through the aperture (spread in time due to multiple ray paths in the box) and to be captured at Port 2 inside the box. When the TRM is applied and $y(-t)$ is re-transmitted from Port 2, the aperture field distribution is reconstructed for the energy to be re-directed to Port 1. In [10], a parametric study was also performed regarding the peak power of the reconstructed pulse as a function of aperture size, pulsewidth (PW) and number of TRM antenna elements. In this paper, we study the spatial and temporal focusing of the time-reversed pulse, whose shape can be arbitrarily defined, through numerical simulation and experiment. Our technique utilizes a much larger bandwidth than Ref. [14], and takes advantage of the complex scattering environment to simplify the experiment by using just a single recording channel in the TRM.

2.2. Linear System Representation of TRM Process

Here we describe the TRM process in terms of a linear time-invariant system and the corresponding impulse response. Considering Ports 1 and 2 as the input and output ports of the system, respectively, the output signal, $y(t)$, can be represented as

$$y(t) = x_i(t) * h_{21}(t) \tag{1}$$

where $x_i(t)$ is the input and $h_{21}(t)$ is the impulse response of the system. The output recorded for a finite time duration of T is represented as

$$y(t;T) = x_i(t) * h_{21}(t;T), \tag{2}$$

where $h_{21}(t;T)$ is now an approximate impulse response between the two ports for a finite time duration of T and represents an approximation to the Green's function that satisfies the wave equation. The usual spatial dependence of the Green's function is not explicitly specified to simplify the notation. Due to the spatial reciprocity in the system, $h_{21}(t)$ remains unchanged when the transport process reverses its direction (i.e. $h_{21}(t) = h_{12}(t)$). When $y(t;T)$ is time-reversed and re-transmitted, the signal received at Port 1 is

$$x_r(t) = y(T-t;T) * h_{21}(t), \tag{3}$$

and the energy is compressed in time to peak around $t = T$, resulting in a pulse very close to a time reversed version of $x_i(t)$. Spatial focusing also occurs at Port 1, such that the amplitude peak of the signal observed at locations other than Port 1 decreases as a function of distance from Port 1, due to the variation of the impulse response function at that location from $h_{21}(t)$. The spatial focal area is diffraction limited and the minimum half-power focal area can be approximated by using the radiated pattern from a rectangular aperture [22], from which a one dimensional resolution is estimated as

$$\Delta_L \cong 0.9D\lambda/A, \tag{4}$$

where D, λ , and A are the distance of Port 1 from the aperture, wavelength, and a dimension (height or width) of the aperture, respectively. This estimate is expected to apply in the far-field. In the near-field, the minimum half-power focal area is approximated by the wavelength squared, which is the diffraction limit for time-reversed wave focusing [23].
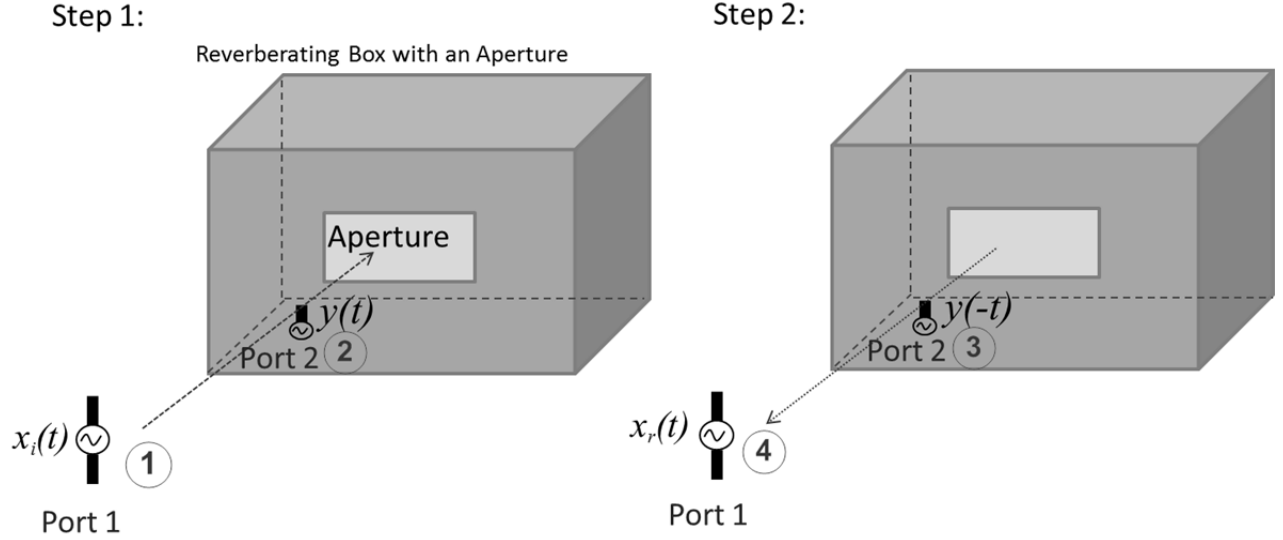
If $x_i(t) = \delta(t)$, then Eqn. (3) becomes

Figure 3. TRM in a reverberating box with an aperture (leaky box)

$$x_r(t) = h_{21}(T - t; T) * h_{21}(t) \qquad (5)$$

where $x_r(t)$ now represents the autocorrelation function of $h_{21}(t)$, which peaks at $t = T$. For locations other than Port 1, $x_r(t)$ simply becomes a cross-correlation function that has a relatively lower peak at $t = T$, since the impulse response of the re-transmission channel differs from the original impulse response. This implies that the TR process can be viewed as a temporal and spatial correlator [23].

2.3 Sending an Arbitrary Pulse

Now we introduce an arbitrary RF pulse, $x_p(t)$. When $x_p(t)$ is convolved with the time-reversed impulse response and transmitted through Port 2, the representation of $x_r(t)$ as in Eqn. (5) is modified to

$$x_r(t) = x_p(t) * h_{21}(T - t; T) * h_{21}(t). \qquad (6)$$

In Eqn. (6), due to temporal compression in the autocorrelation term, the original pulse shape of $x_p(t)$ is preserved and peaks around $t = T$. The essence of this approach lies in the time-reversal impulse response, which is capable of undoing the phase changes and distortions at all frequencies. Therefore, when convolved with an arbitrary RF pulse and transmitted from Port 2, the RF pulse will be effectively delivered to Port 1

in its original pulse shape. Spatial focusing of the peak power should also take place at Port 1 in the same manner as previously mentioned. Figure 3 shows a modified illustration of the TRM in a leaky box using the time-reversal impulse response concept. From a practical perspective, where the "impulse response" has a finite bandwidth due to the pulse width of the excitation pulse, as well as the bandwidth of transmit and receive system (i.e. ports, reverberating box), the frequency bandwidth of an arbitrary RF pulse must be within the spectrum of the impulse response.

3. Numerical Simulation

A model of the reverberating box with an aperture was simulated using SEMCAD®, a Finite Difference Time Domain based computer code. As shown in Figure 4, the dimensions of the box were 1.8m×1.2m×1.1m (W×H×L). The aperture was placed on the broad side of the box with dimensions of 1m×0.4m (WA×HA). The box parameters used in the model are similar to those used in [14]. Port 1 was modeled as a fat dipole, and is located at a distance of 1.5m from the aperture and 0.55m to the right of the boresight axis. Along the plane perpendicular to the boresight axis at 1.5m from the aperture, sensors were placed to record the signal at locations other than Port 1 to examine the degree of spatial focusing. Port 2 (TRM) was modeled as a monocone antenna and is located on the
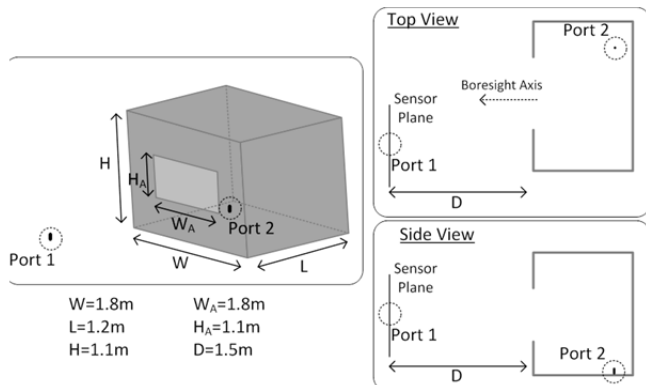

Figure 4. Numerical simulation setup of the TRM in a reverberating box with an aperture.
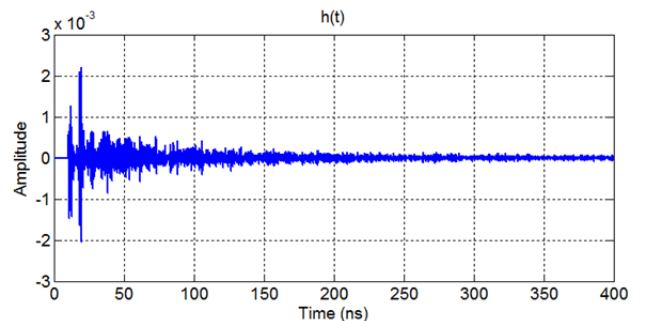

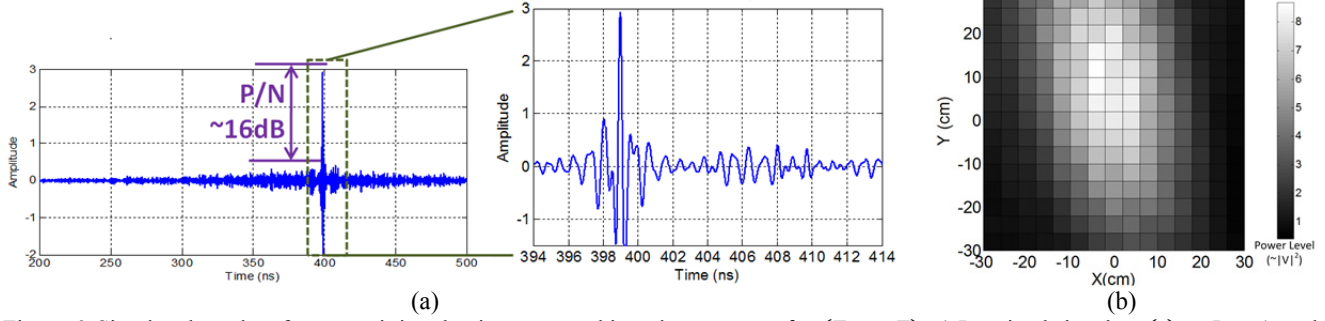Figure 5. Simulated impulse response, $h_{21}(t; T)$, at Port 2.

Figure 6. Simulated results of retransmitting the time-reversed impulse response, $h_{21}(T - t; T)$: a) Received signal, $x_r(t)$, at Port 1, and b) Peak values recorded across the sensor plane (perpendicular to the boresight direction), where the location of Port 1 is (0,0).

bottom inside, near the back left corner of the box. The walls of the box were assumed to be perfectly conducting.

The approximate impulse response, $h_{21}(t; T)$, was simulated by transmitting a 300ps Gaussian pulse from Port 1, and recording the response at Port 2 for T=400ns (see Figure 5). $h_{21}(t; T)$ was then time reversed and retransmitted from Port 2, and the signals were recorded at Port 1 and along the sensor plane to examine the temporal (reconstruction of the short pulse) and spatial focusing. Figure 6a shows the signal received at Port1, which corresponds to $x_r(t)$ in Eqn. (5). In the figure, a short pulse that peaks near t=T with the pulse width of 300ps, which resembles the original pulse, is observed with the peak to "noise" ratio, P/N, of ~15dB, indicating a good temporal compression of the TR impulse response. Note that the signal amplitude is not quantified, since the purpose of this paper is to examine the focusing properties in a relative sense. In Figure 6b, the peak power levels ($\max\{|x_r(t)|^2\}$) recorded across the planar sensors are shown. Spatial focusing is clearly observed around the Port 1 location (x = y = 0), with the half-power focal area of approximately 0.3x0.4m^2.

Next, a particular RF pulse, $x_p(t)$, of 5ns PW at 2.3GHz frequency was chosen and convolved with the time-reversed impulse response, $h_{21}(T - t; T)$. The convolved signal, $x_p(t) * h_{21}(T - t; T)$, was then transmitted from Port 2 and recorded at Port 1. The reconstructed signal, $x_r(t)$, resembles a time-reversed version of $x_p(t)$ with good fidelity. The spatiotemporal focusing achieved by the signal received at Port 1 is summarized in Table 1, along with experimental results.

4. Experiment

Measurements were made with a reverberating box with an aperture placed in a large anechoic chamber as shown in Figure 7. The dimensions of the box were 1.22m×1.27m×0.65m (W×H×L). The TRM (Port 2) in the box was a small monocone antenna placed in the bottom of the box left of center. The aperture dimensions were 0.7m×0.4m (W$_A$×H$_A$). At a distance of 1.9m from the aperture in the boresight direction, an ultra-wideband antenna was placed in a 2D scanner to measure the response at different locations. The original Port 1 location was set to 0.5m above and 0.4m to the right of the boresight axis. In this experiment, a network analyzer was used to measure the S$_{21}$ frequency response (from 0.01-15GHz) between the ports. The measured frequency response is the frequency response of the cavity compounded with that of the antennas. The frequency response was then inverse Fourier

transformed into the time domain to obtain the approximate time-domain impulse response. The frequency step was set to 2.34MHz, which yielded the equivalent record time, T, of about 427ns.

The retransmission of the TR signals ($h_{21}(T - t; T)$ or $x_p(t) * h_{21}(T - t; T)$) in their full bandwidth requires an arbitrary waveform generator with a sufficient bandwidth. However, due to the lack of an arbitrary waveform generator with such bandwidth, we have estimated the reconstructed signals in Eqns. (5) or (6) by utilizing the measured channel transfer function (S_{21} response). In other words, we have predicted the outcome of the time reversal experiment by convolving the TR signals with the measured impulse response between the TRM and the scanned positions including the source location. The spatial reciprocity in the experiment should allow for the predicted outcome to be an accurate estimate of the actual reconstructed signal.
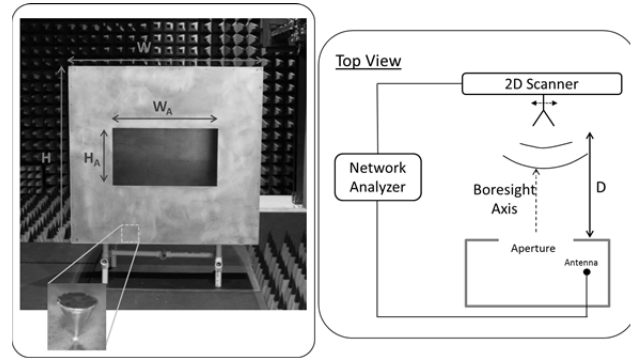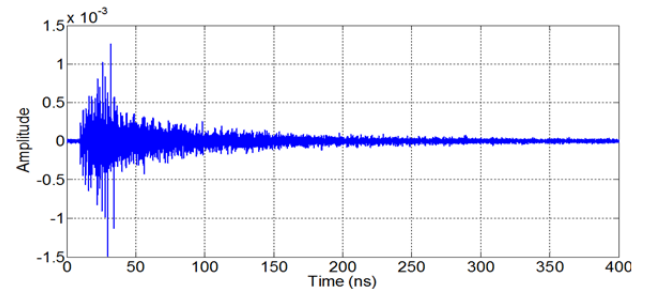

Figure 7. Measurement setup.

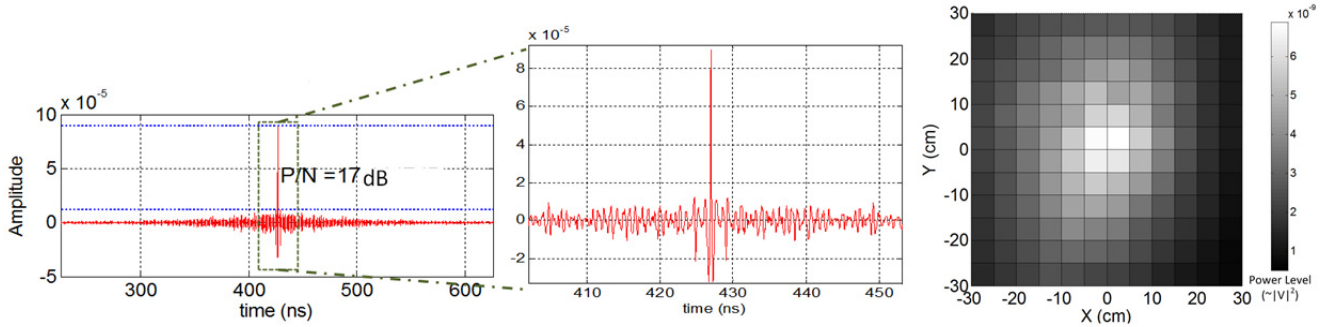Figure 8. Experimental impulse response, $h_{21}(t; T)$, obtained from the frequency response (10MHz-15GHz).

Figure 9. Experimental results of estimating the retransmission of the time-reversed impulse response, $h_{21}(T - t; T)$: a) Reconstructed signal $x_r(t)$ at Port 1, and b) Peak values recorded at different positions of planar scanner (perpendicular to the boresight direction), where the location of Port 1 is (0,0).

Table 1. Comparison of numerical and experimental results. Figures 6 and 9 illustrate representative numerical and experimental results summarized in this table. $T \approx 400$ns for all cases. (The minimum focal area in the near field is estimated by using the square of the wavelength. This considers the diffraction limit for time-reversed wave focusing [23]. †††)

	Signal Transmitted from TRM	Carrier Freq. (GHz)	RF Pulse Width (ns)	Wavelength (m)	D (m)	$W_A \times H_A$ (m×m)	P/N (dB)	Estimated Minimum Focal Area (m×m) Eqn. (4)	Obtained Focal Area (m×m)
Numerical	$h_{21}(T - t; T)$	2.2	N/A	0.14	1.5	1.0×0.4	15	0.18×0.46	0.3×0.5
	$x_p(t) * h_{21}(T - t; T)$	2.3	5	0.13	1.5	1.0×0.4	10	0.18×0.45	0.2×0.5
Experimental	$h_{21}(T - t; T)$	7	N/A	0.043	1.9	0.7×0.4	17	0.11×0.18	0.2×0.3
	$x_r^1(t) * h_{21}(T - t; T)$	7	5	0.043	1.9	0.7×0.4	10	0.11×0.18	0.15×0.2
	$x_r^2(t) * h_{21}(T - t; T)$	9	5	0.033	1.9	0.7×0.4	11	0.03×0.03 †††	0.11×0.15
	$x_r^3(t) * h_{21}(T - t; T)$	3	20	0.1	1.9	0.7×0.4	9	0.25×0.43	0.3×0.45

The impulse response, $h_{21}(t; T = 427\text{ns})$, obtained from the network analyzer measurement is shown in Figure 8. The estimated $x_r(t)$ at Port1 is shown in Figure 9a, where an impulse-like signal that peaks near $t = T$, is observed with P/N of ~17dB, indicating a good temporal compression. Note again that the signal amplitude is not quantified. Figure 9b shows the peak power levels $(\max\{|x_r(t)|^2\})$ at different locations of the 2D scanner. Spatial focusing is clearly observed around the original Port 1 location with the half-power focal area of approximately 0.3m×0.3m. This measurement area is chosen to be larger than the square of most of the wavelengths within the bandwidth of the impulse response. This allowed us to observe the spatial focusing clearly as shown in Figure 9b.

For examples of arbitrary RF pulses, three different signals, i.e. 1.) $x_p^1(t) = 7$ GHz with 5 ns PW, 2.) $x_p^2(t) = 9$ GHz with 5ns PW, and 3.) $x_p^3(t) = 3$ GHz with 20ns PW, were used. Each RF pulse was convolved with the time-reversed impulse response, $h_{21}(T - t; T)$. The resulting signal was then convolved again with the corresponding impulse responses at each scanned position to estimate the reconstructed signal, $x_p^1(t)$, $x_p^2(t)$, and $x_p^3(t)$ for each respective RF pulse, as summarized in Table 1. In all cases, a pulsed RF that resembles the original signal is observed at $t = T$, with reasonable P/N values. Spatial focusing occurred near Port 1 for all cases, and the focal area is found to be proportional to the wavelength (inversely proportional to the RF frequency) as expected - i.e., 0.3x0.45m², 0.15x0.2m², 0.11x0.15m², for 3, 7, and 9 GHz,

respectively. For $x_p^3(t)$, the estimated $x_r^3(t)$ does not seem to resemble the original pulse as closely as in other cases, which indicates a relatively poorer temporal compression.

In Table 1, the minimum focal area is estimated using two techniques. For 3 GHz and 7 GHz, the far-field condition, and hence the use of Eq. (4) is justified. Because, Port 1 is within the far-field of the aperture at 3GHz. At 7GHz, Port 1 is actually within the radiative near-field region of the aperture, but the far-field term ($1/r$ term) is dominant enough, such that the far-field aperture diffraction limit can still be applied. On the other hand, for the experiment with 9GHz, Port 1 is not within the far field, and Eq. (4) could not be applied; instead, the minimum focal area was estimated as the square of the wavelength [23]. It should be noted, however, that t

5. Discussion

5.1 Comparison of the Results

Table 1 shows a comparison of the simulation and experimental results discussed so far. In the table, the estimated minimum spatial focal area using Eqn. (4) is also shown. For the impulse responses (results shown in Figures 6 and 9), the minimum focal area was estimated using the center frequency of the impulse bandwidth. Also notice that the estimated and observed focal area are not as close as those from the pulsed RF results, since Eqn. (4) only estimates the focal area at one frequency. In all cases the observed focal area is slightly larger than the estimated minimum, due to some approximations used in Eqn. (4) (i.e.

based on a uniform aperture distribution and Δ_L approximated from the arc length of the half-power angle in the aperture radiation pattern) and the port 1 location being off the boresight axis (i.e. the beamwidth broadens when off the boresight). Note that in all cases the focal area is elongated along the direction that is expected based on the shape of the rectangular aperture. Overall, the results are promising and indicate that reasonable temporal and spatial focusing of an arbitrary RF pulse can be achieved through the use of a time-reversed impulse response.

5.2 Pulse Quality

As previously mentioned, the quality of the reconstructed pulse is largely determined by losses in the process. In this particular case the loss is mainly caused by: 1) the energy lost in the radiation (never captured by the aperture), 2) the energy lost through the aperture during reverberation in the box, 3) finite duration of the recorded impulse response, and 4) the conductor loss in the cavity walls and the ports.

By reducing the loss in the process, a better reconstruction may be achieved, particularly improving the P/N. One way to do so is to reduce the size of the aperture. It was shown in [14] that the aperture area of $\sim\lambda^2$ gives the best temporal compression at a given frequency. However, a smaller aperture size results in a larger spatial focal area due to the diffraction limit. Moreover, the electrical size of the aperture varies with frequency. Hence it would be important to determine the parameters that provide optimal temporal and spatial focusing over the frequency band of interest. For the reverse problem (focusing the energy at a target in an enclosure), selecting an optimal frequency band for an effective focusing for given parameters would be of interest. On the other hand, the spatial focusing area can be controlled using the wavelength if all other conditions are the same.

One of the loss mechanisms discussed above is the finite duration of the recorded impulse response. This limitation can be overcome by using the so called closed time reversal mirror [24]. The closed time reversal mirror has an ideal comprehensive spatial coverage using an infinite number of antennas. The closer the system is to the closed time reversal mirror, the better the focusing quality. The ray chaotic nature of the reverberation chamber results in a wave pattern with multiple polarizations regardless of the polarization of the initial signal broadcast. Therefore, having an antenna system that can pick up signals in more than one polarization direction is also expected to improve the performance of the time reversal mirror. Both of the antennas used in this experiment were vertically polarized.

Another limitation of the experiment involves the fact that only the wave field is measured even when the aperture of the reverberation chamber is within the near field of the TRM. Based on Ref. [15], both the wave field and the normal derivative of the wave field need to be measured when time reversal is done in the near field of a source; our experiment has a limitation because only the wave field is measured.

6. Summary and Conclusions

In this paper, we presented a technique to effectively send an arbitrary RF pulse at a region at a distance from a single aperture using time reversal. Utilizing a TRM in a leaky cavity, we showed that when the time-reversed impulse response is convolved with an arbitrary RF pulse and transmitted through the TRM, an effective delivery of that pulse to the target location takes place. Numerical simulation and laboratory measurements were conducted to examine temporal and spatial focusing of the pulse at Port 1 using RF pulses of different center frequencies and pulse-widths. In all cases, a good temporal compression occurred at time $t = T$ (the record length of the signal) as expected, with the signal $x_r(t)$ closely resembling a time-reversed version of the original pulse. Spatial focusing was also observed with the focal area in agreement with estimates based on the diffraction limit. It was clearly seen from the results that an RF pulse can be effectively delivered using the TRM if the impulse response between the desired location and the TRM can be obtained.

We have shown that we can deliver an RF pulse of choice using the impulse response for a given target location or direction. This approach could be an efficient selective "beamforming" method for directed energy over an ultra-wide bandwidth, where it only requires a single feed and the pre-stored (or obtained on-the-fly) impulse response between the TRM and target location or direction to effectively deliver an RF pulse of choice. Alternatively the system can be used as well to focus energy at a targeted location in an enclosure that has one or more entry points for electromagnetic energy. One limitation of this method is that the spatial focusing of the signal in a scenario similar to that depicted in Figure 1b will be limited by the aperture size. However the peak field created in the reconstructed pulse has been shown to be independent of the aperture size [14].

Currently under investigation are techniques to improve the quality of the reconstructed pulse in terms of pulse shape, P/N (temporal focusing) and the spatial focusing. Examining different TRM parameters and structures (i.e. a ray-chaotic box, different aperture profile), as well as different TR pre-processing are also under investigation and will be the subject of future publications.

References

[1] Lerosey G, de Rosny J, Tourin A, Derode A, Montaldo G, Fink M. Time reversal of electromagnetic waves. Physical Review Letters. 2004;92:193904.
[2] Lerosey G, de Rosny J, Tourin A, Derode A, Fink M. Time reversal of wideband microwaves. Physical Review Letters. 2006;88:154101.
[3] Nguyen HT, Andersen JB, Pedersen GF. Potential use of time reversal techniques in multiple antenna systems. IEEE Communications Letters. 2005;9(1):40-42.
[4] Xiao SQ, Chen J, Wang BZ, Liu XF. A numerical study on time reversal electromagnetic wave for indoor ultra-wideband signal transmission. Progress in Electromagnetic Reserarch. 2007;77:329-342.
[5] Wang D, Wang BZ, Ge GD, Chen ST, Tang MC. The feasibility of envelope-based time reversal. Journal of Electromagnetic Waves and Applications. 2011;25:63-74.

[6] Jin Y, Moura JMF, O'Donoughue N. Adaptive time reversal beamforming in dense multipath communication networks. 42nd Asilomar Conference on Signals, Systems and Computers. 2008 October 26-29; Pacific Grove, CA.

[7] Dezfooliyan A, Weiner AM. Experimental test-bed for studying multiple antenna beamforming over ultra wideband channels up to 12GHz. IEEE Wireless Communications Letters. 2012;1(5):520-523.

[8] Chen GP, Yu WB, Zhao ZQ, Nie ZP, Liu QH. The prototype of microwave-incuded therno-acoustic tomography imaging by time reversal mirror. Journal of Electromagnetic Waves and Applications. 2008;22:1565-1574.

[9] Kosmas P, Rappaport C. Time reversal with the FDTD method for microwave breast cancer detection. IEEE Transactions on Microwave Theory and Techniques. 2005;53(7):2317-2323.

[10] Anlage SM, Rodgers J, Hemmady S, Hart J, Antonsen TM, Ott E. New results in chaotic time-reversed electromagnetics: high frequency one-recording-channel time reversal mirror. Acta Physica Ponolica A. 2007;112:569-574.

[11] Taddese BT, Hart J, Antonsen TM, Ott E, Anlage SM. Sensor based on extending the concept of fidelity to classical waves. Applied Physics Letter. 2009;95:114103.

[12] Taddese BT, Hart J, Antonsen TM, Ott E, Anlage SM. Sensing small changes in a wave chaotic scattering system. Journal of Applied Physics. 2010;108:114911.

[13] Taddese BT, Antonsen TM, Ott E, Anlage SM. Iterative time reversal with tunable convergence. Electronic Letters. 2011;47(21):1165-1167.

[14] Davy M, de Rosny J, Fink M. Focusing and amplification of electromagnetic waves by time reversal in a leaky reverberation chamber. Comptes Rendus Physique. 2010;11(1):37-43.

[15] Fink M, Cassereau D, Derode A, Prada C, Roux P, Tanter M, Thomas JL, Wu F. Time-reversed acoustics. Reports on Progress in Physics. 2000;63(12):1933-1995.

[16] Ciattaglia M, Marrocco G. Time domain synthesis of pulsed arrays. IEEE Transactions on Antennas and Propagation. 2008;56(7):1928-1938.

[17] Aulbach J, Bretagne A, Fink M, Tanter M, Tourin A. Optimal spatiotemporal focusing through complex scattering media. Physical Review E. 2012;85:016605.

[18] Yun Z, Iskander MF. Time reversal with single antenna systems in indoor multipath environments: spatial focusing and time compression. IEEE International Antenna and Propagation Symposium. 2006 July 9-14; Albuquerque, NM.

[19] Parihar DPS, Agarwal A, Agarwal M. Time reversal mirror: temporal and spatial focusing tool. OCEANS 2010 IEEE. 2010 May 24-27; Sydney, Australia.

[20] Montaldo G, Aubry JF, Tanter M, Fink M. Spatio-temporal coding in complex media for optimum beamforming: the iterative time-reversal approach. IEEE Transactions of Ultrasonics, Ferroelectrics and Frequency Control. 2005;52(2):220-230.

[21] Frazier M, Taddese B, Antonsen T, Anlage SM. Nonlinear time reversal in a wave chaotic system. Physical Review Letters. 2013;110:063902.

[22] Stutzman WL, Thiele GA. Antenna theory and design. 2nd ed. Hoboken (NJ): Wiley; 1998.

[23] Lerosey G, de Rosny J, Tourin A, Fink M. Focusing beyond the diffraction limit with far-field time reversal. Science. 2007;315(5815):1120-1122.

[24] Cassereau D, Fink M. Time-reversal of ultrasonic fields .3. theory of the closed time-reversal cavity. IEEE Transactions of Ultrasonics, Ferroelectrics and Frequency Control. 1992;39(5):579-592.